JOURNAL OF MATERIALS SCIENCE 19 (1984) 1737–1748

The optical absorption edge of amorphous thin films of silicon monoxide

S. K. J. AL-ANI, K. I. ARSHAK, C. A. HOGARTH
Department of Physics, Brunel University, Uxbridge, Middlesex, UK

The absorption edges of vacuum-evaporated silicon monoxide films are studied and a general equation based on the absorption being due to non-direct electronic transitions in k-space is found to be compatible with the experimental results. The optical energy gap, E_{opt}, is determined from the high absorption region of the fundamental edge. Measurements on films deposited at different rates and having different thicknesses are analysed and discussed in terms of the values of E_{opt}. The form of the absorption edge remains similar for annealed films but annealing has the effect of increasing the values of E_{opt}. The experimental results are related to earlier published work based on measurements of electron spin resonance and refractive index of films prepared under different conditions and additional experiments are reported.

1. Introduction

Amorphous non-metallic materials exhibit absorption edges which are less abrupt and well-defined than for materials having the corresponding crystalline form. Nevertheless, measurements of optical absorption edges have helped considerably in developing an understanding of the theory of electronic structures of amorphous materials, given the theoretical bases laid by Tauc [1], Davis and Mott [2] and others. According to Tauc the absorption edge of an amorphous solid can be classified into three parts as shown in Fig. 1.

(a) a high-energy region (part a, in Fig. 1, where the absorption coefficient $\alpha > 10^4\,cm^{-1}$) in which α is described by an equation of the form

$$\alpha\hbar\omega = B'(\hbar\omega - E_{opt})^n \qquad (1)$$

where ω is the angular frequency of the radiation, B' is a constant, E_{opt} is the optical energy gap and n has a value between 1 and 3. According to Tauc and his colleagues [3, 4], providing that energy is conserved during the absorption process and that the density-of-states function for nonlocalized states is parabolic, the absorption coefficient is defined by an equation

$$(\alpha\hbar\omega)^{1/2} = B(\hbar\omega - E_{opt}). \qquad (2)$$

However, the density-of-states functions may not be parabolic and indeed Davis and Mott [2] made the assumption that at the band edges they are linear functions of energy. Nevertheless, they also proposed an equation of the same form as Equation 2 for absorption by non-direct transitions.

(b) The absorption coefficient between 1 and $10^4\,cm^{-1}$ (part b, Fig. 1) increases exponentially with photon energy $\hbar\omega$ and may be described by the following relation

$$\alpha(\omega)\alpha\exp(\hbar\omega/E_1). \qquad (3)$$

The energy E_1 characterizes the steepness of the exponential tail of the density-of-states curve as it defines the localized states and indeed the Urbach rule [5] is interpreted by assuming that E_1 measures the width of the tail of localized states in the band gap.

(c) The absorption coefficient below $1\,cm^{-1}$ (part c, in Fig. 1) may also be determined by a relation of the same form as Equation 3 above but with a larger energy E_2. Tauc *et al.* [6] assumed that this low energy tail was probably an intrinsic feature of the material and we shall not discuss it further.

Equation 2 has been applied by many workers for the analysis of optical absorption edge data, for example by Mott and Davis [7] and by Moridi and Hogarth [8], for chalcogenide and oxide glas-

0022–2461/84 $03.00 + .12

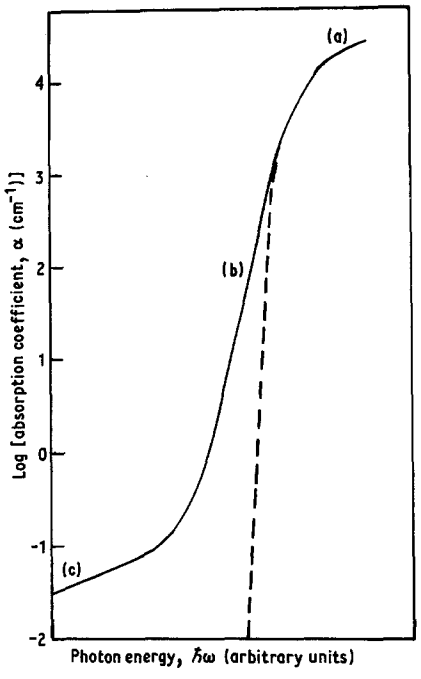

Figure 1 The general shape of the absorption edge of amorphous semiconductors. (The broken line represents extrapolation of part a.)

ses, respectively. Recently, Hogarth and Nadeem [9] applied the same equation to the absorption edge of the thin amorphous oxide film consisting of GeO_2 and also samples containing BaO. Realistic values of E_{opt} were derived and a systematic variation with added BaO was observed.

We have made a series of SiO films and have studied their optical absorption edges and shown how the derived values of E_{opt} depend on the conditions of preparation, thickness, annealing and other parameters. We have attempted to explain our results in terms of disorder and consequential band tailing. SiO was chosen partly because of its importance as a practical material [10, 11] and partly because the properties of both Si and SiO are known to depend very sensitively on the conditions of preparation. Indeed serious articles have been published, for example by Beynon [12], which suggest that SiO in thin film form may not actually exist, and in principle could consist of an intimate fine granular aggregate of Si and SiO_2. We have related our results to earlier papers of Philipp [13] who had studied the absorption edge of silicon oxides somewhat less extensively and of Timson and Hogarth who had reported ESR measurements on thin SiO films [14].

2. Experimental work

2.1. Specimen preparation

Thin films of SiO were prepared by vacuum evaporation from a tantalum boat 1 mm thick in a Balzers 510 Coating Unit. Using the liquid nitrogen trap, the ultimate pressure was $\sim 10^{-7}$ torr, rising to $\sim 10^{-6}$ torr during the thermal evaporation process. Corning glass 7059 slides were used for the substrates and were thoroughly cleaned in a series of well-known steps before use. Various rates of evaporation, R, between 0.7 and 10 nm sec^{-1} were used.

A quartz crystal thickness monitor was placed close to the substrate at a distance of 25 cm from the source and gave an indication of the film thickness during deposition. The actual thicknesses of the films studied were determined by multiple-beam interferometry using Fizeau fringes of equal thickness.

A radiant heater was incorporated into the bell-jar assembly and used for baking out the system and improving the ultimate vacuum, and also for substrate heating and for annealing treatments. The substrate temperature was monitored using a chromel–alumel thermocouple attached to the top of the substrate.

In order to establish a more systematic scheme for studying the thickness dependence of properties, a moving shutter was designed and built to give fixed thicknesses in sequence during a given evaporation run as indicated in Fig. 2. Six isolated specimens of successively increasing thickness could be made on a single Corning substrate and as closely as possible were prepared under identical conditions of pressure, temperature, deposition rate and so on. A typical sample area was 250 mm^2 with a maximum thickness of 1 μm.

2.2. Optical and electron spin resonance measurements

The optical absorption measurements were made using a Perkin–Elmer Model 402 spectrophotometer. The double-beam system enabled the absorption due to the substrate alone to be subtracted from the absorption due to substrate plus film and a value for the film alone to be estimated. For very thin films and in spectral ranges where the absorption is high, this procedure could possibly be rather insensitive and inaccurate. It was established that the absorption in the Corning glass substrates was low and that the double-beam substrate compensation technique was suitable for our

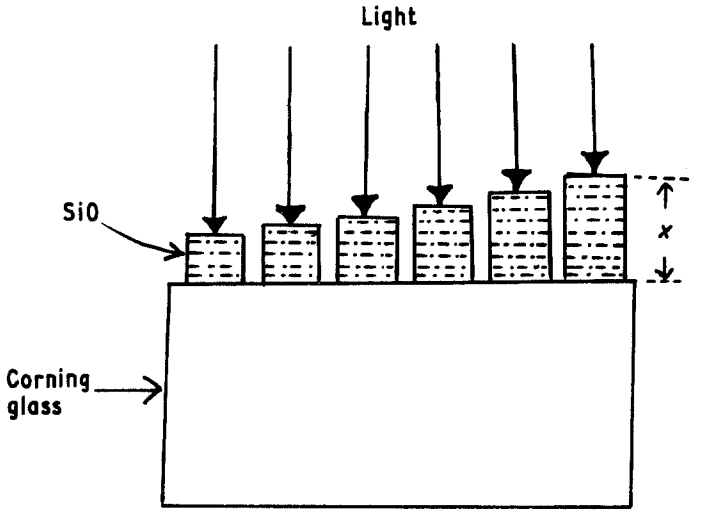

Figure 2 Vertical segment (expanded scale) of sample used to determine thickness variation of absorption.

proposed measurements. The spectral range covered was from the ultraviolet through the visible (190 to 850 nm) regions. Measurements were made at room temperature using a slit width of 25 μm and a fast scan.

The measurements of infrared (IR) absorption were made using a modified technique. A disc of KBr of 2 cm diameter was prepared by hot pressing and its IR absorption spectrum was measured using a Perkin–Elmer 577 grating infrared double-beam spectrometer. A thin SiO film was then deposited on the KBr disc and the new spectrum recorded.

The ESR measurements were made using a Varian E-3 EPR spectrometer working near 3 cm and used well-known standard procedures. The absorption was calibrated using a solution of copper sulphate.

3. Results and discussion

Figs. 3 and 4 show the absorption spectra near the fundamental edge for a series of evaporated SiO samples of different thicknesses but deposited on one substrate. The absorption coefficient α is obtained from the standard relation

$$\alpha = x^{-1} \ln (I_0/I_t)$$

where I_0 is the intensity of incident light after cor-

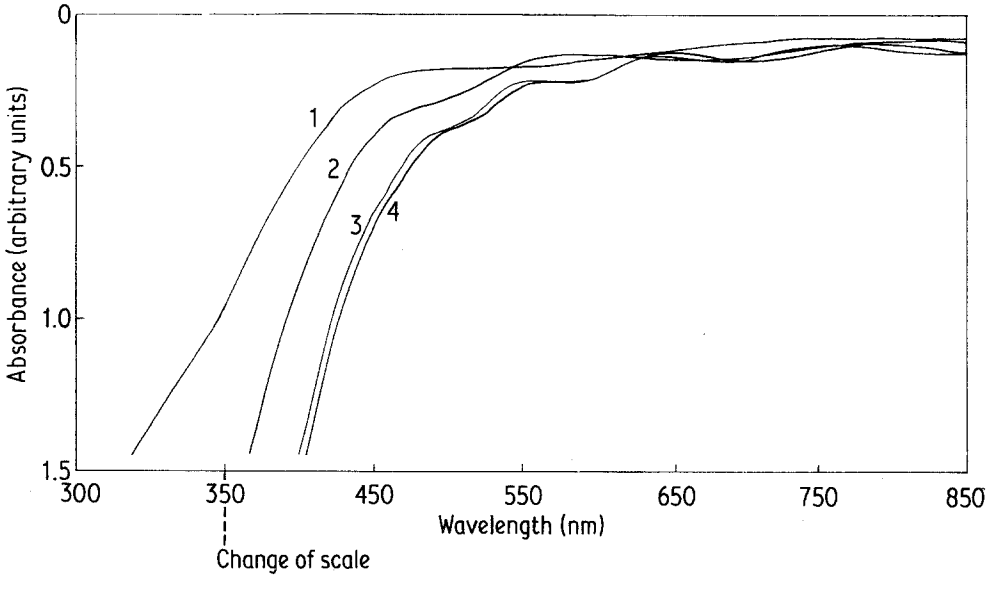

Figure 3 Absorption spectra as a function of wavelength for SiO samples of different thickness following deposition at a rapid rate (1) 177 nm; (2) 370 nm; (3) 655 nm; (4) 770 nm.

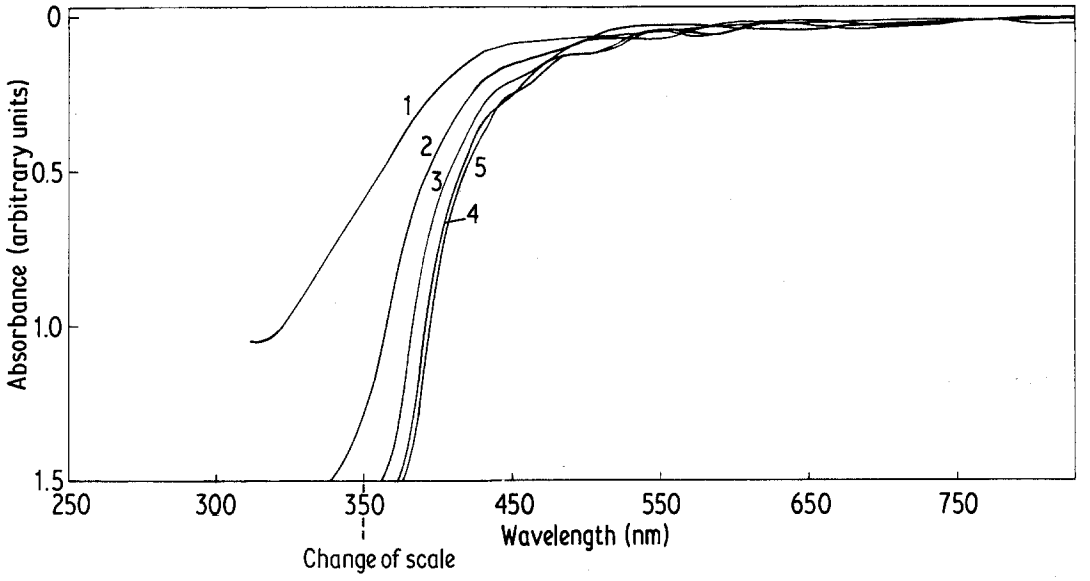

Figure 4 Absorption spectra as a function of wavelength for SiO samples of different thickness following deposition at a slower rate. (Spectrum for sample 1 was not recorded for $\lambda < 310$ nm because of strong substrate absorption.) (1) 210 nm; (2) 365 nm; (3) 583 nm; (4) 745 nm; (5) 852 nm.

recting for reflection and I_t is the intensity of light after traversing a thickness x of the sample material. The high absorption region in Figs. 3 and 4 may be regarded as (a) in Fig. 1 and may be analysed by plotting $(\alpha\hbar\omega)^{1/2}$ against $\hbar\omega$ in accordance with Equation 2. The results are shown in Figs. 5 and 6 and are of linear form in the high absorption region since the matrix element for optical transitions remains constant. The values of E_{opt} obtained from extrapolation of the linear regions and of B obtained from the slopes of the derived curves of the form shown in Figs. 5 and 6, are given in Table I. The mean values of E_{opt} for SiO prepared under the conditions described in Section 2 are 2.25 ± 0.03 eV for a rapid rate of evaporation R and 2.73 ± 0.02 eV for a slow rate of evaporation. The tail in the curves of the type given in Figs. 5 and 6 may be regarded as the exponential absorption tail corresponding to (b) in Fig. 1. In this region it is convenient to fit the experimental data to an empirical formula due to Urbach [5] similar in form to Equation 3. Such plots for our samples as given in Figs. 7 and 8 and the values of E_1 in Equation 3 lie in the range 0.50 to 0.42 eV and 0.35 to 0.27 eV for rapid and slow evaporations, respectively. Different suggestions about this tail have been made. Tauc [17] believes that the exponential variation of α with $\hbar\omega$ is due to transitions between localized states and will vary from sample to sample. Davis and Mott [2] assume that the value of E_1 will be much the same for most amorphous semiconductors and indeed values for chalcogenide glasses are reported to lie between 0.46 and 0.066 eV. Moridi and Hogarth found the values of E_1 for copper–calcium–phosphate glasses to lie in the range 0.66 to 1.06 eV depending on copper concentration, and other values larger than those suggested for the chalcogenide glasses by Davis and Mott have been found for other oxide glasses.

TABLE I E_{opt} and the constant B for SiO films of different thicknesses, evaporated at pressure of $\sim 10^{-6}$ torr

Sample	Thickness (nm)	E_{opt} (eV)	$B \times 10^{-5}$ ($cm^{-1} eV^{-1}$)
(i) *Rapid evaporation*			
1	177	2.27	2.71
2	370	2.30	2.50
3	655	2.23	2.07
4	770	2.20	1.87
(ii) *Slow evaporation*			
1	210	2.70	3.23
2	365	2.75	5.27
3	583	2.75	8.79
4	745	2.72	4.90
5	852	2.73	5.10

The amorphous nature of the films was confirmed by X-ray and electron-microscope examination. It may be seen from Figs. 5 and 6 that the absorption coefficient and the factor $(\alpha\hbar\omega)^{1/2}$ always increase as the thickness of the film

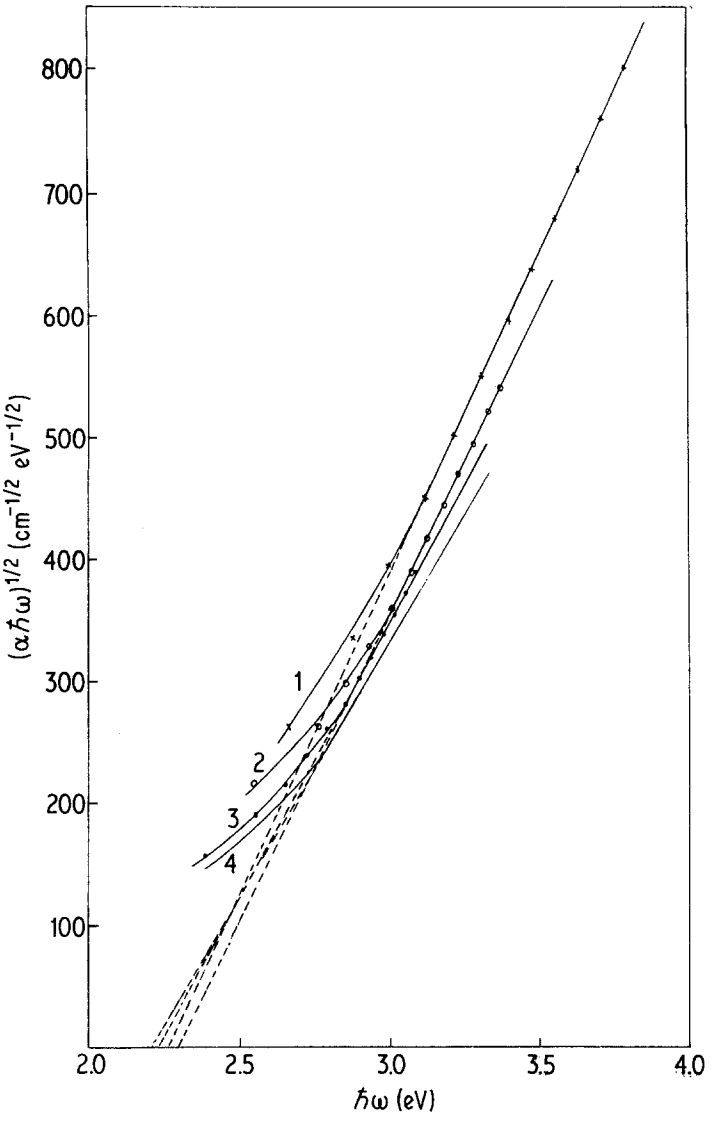

Figure 5 Data of Fig. 3 replotted in terms of the theories of Tauc and of Davis and Mott.

decreases. The large value of the absorption coefficient for small thickness may be due to a high transition probability of carriers across the relevant E_{opt} between the localized states [15].

The annealing was carried out for 4 h at 500 K in a vacuum of 5×10^{-6} torr followed by cooling to room temperature at a rate of $1^\circ C\,min^{-1}$. The shapes of the absorption edges for annealed silicon monoxide display approximately the same properties, but they shift to shorter wavelengths and so the values of E_{opt} in general increase. Figs. 9 and 10 and Table II show the results for both rapid and slow evaporation.

The variation of E_{opt} with thickness may be explained as follows. Some dangling bonds (un-

TABLE II The influence of annealing on the optical energy gap of some silicon monoxide films

x (nm)	Before annealing		After annealing	
	E_{opt} (eV)	$B \times 10^{-5}$ ($cm^{-1}\,eV^{-1}$)	E_{opt} (eV)	$B \times 10^{-5}$ ($cm^{-1}\,eV^{-1}$)
(i) *Rapid evaporation*				
177	2.27	2.71	2.35	3.23
370	2.30	2.50	2.40	2.99
655	2.23	2.07	2.37	2.68
770	2.20	1.87	2.31	2.24
(ii) *Slow evaporation*				
422.5	2.72	5.74	2.74	6.10
605.0	2.74	6.02	2.79	6.46
730.0	2.75	6.42	2.75	5.92
773.0	2.79	7.65	2.77	6.94
850.0	2.79	7.90	2.79	6.94

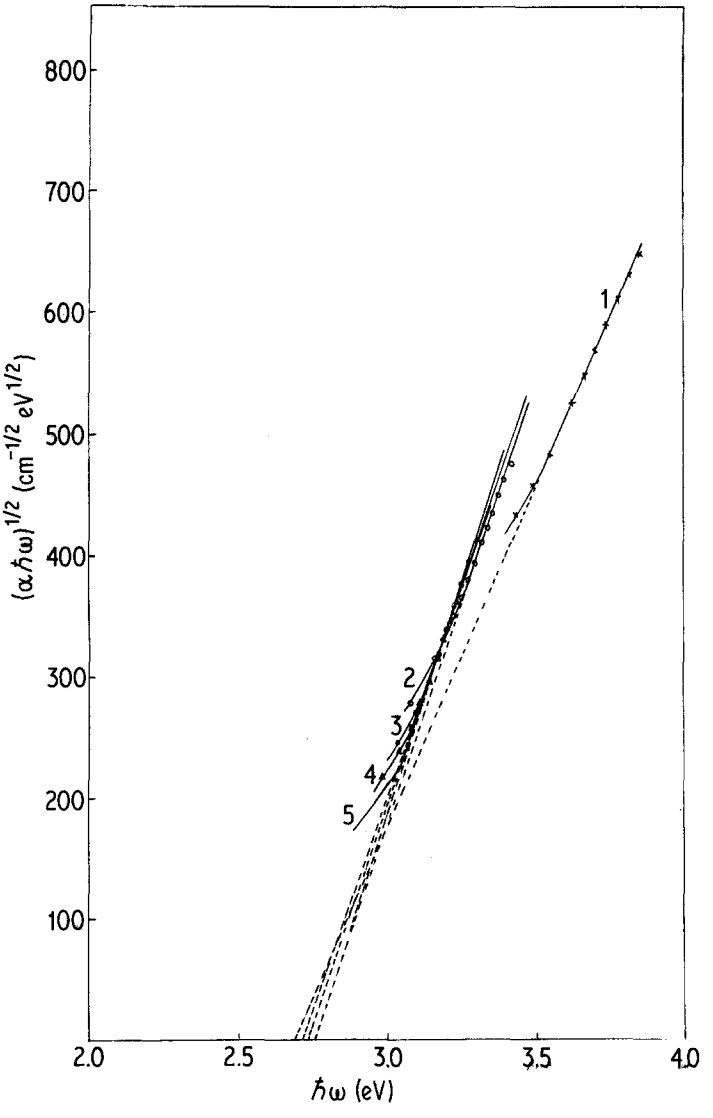

Figure 6 Data of Fig. 4 replotted in terms of the theories of Tauc and of Davis and Mott.

saturated) are likely to be created at the beginning of the deposition process and these would be expected to act as structural defects which are responsible for the localized states in the material. Increasing the thickness by successive evaporations, a somewhat more homogeneous amorphous network is built up with a less open structure, thus reducing to some extent the dangling bonds, the proportion of defects and the concentration of localized states. Thus a nearly ideal amorphous sample may be reached and the value of E_{opt} approaches asymptotically its limiting value.

Similarly, during the annealing process the film will have time for some atomic re-arrangement to take place, some defects will be removed which, reducing the density of dangling bonds, redistribute atomic distances and bond angles, and E_{opt} will then increase and tend asymptotically towards some limiting value.

The infrared absorption spectra of KBr and of KBr carrying a thin SiO film are shown in Fig. 11 and the peak absorption in the vicinity of 10 μm is charactersitic of SiO [16].

The ESR measurements of Timson and Hogarth [14] have been repeated and our recent measurements on samples made under identical conditions to those for the optical measurements are given in Fig. 12 where the spin density is plotted as a function of R/p where R is the rate of evaporation and p is the pressure during the evaporation process. Our recent refractive index measurements are given in Fig. 13 and again seen to follow the curves

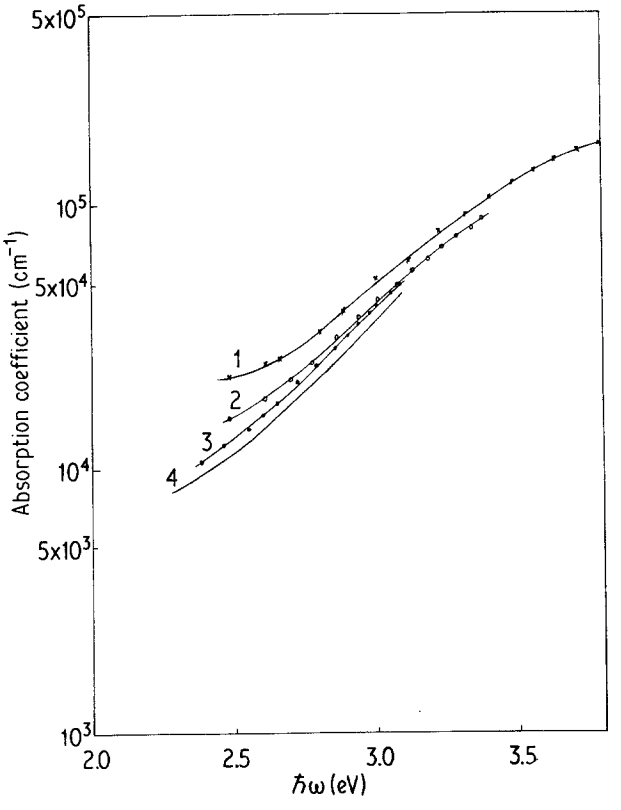

Figure 7 Absorption coefficient as a function of photon energy for rapidly evaporated SiO films. (Data of Fig. 3)

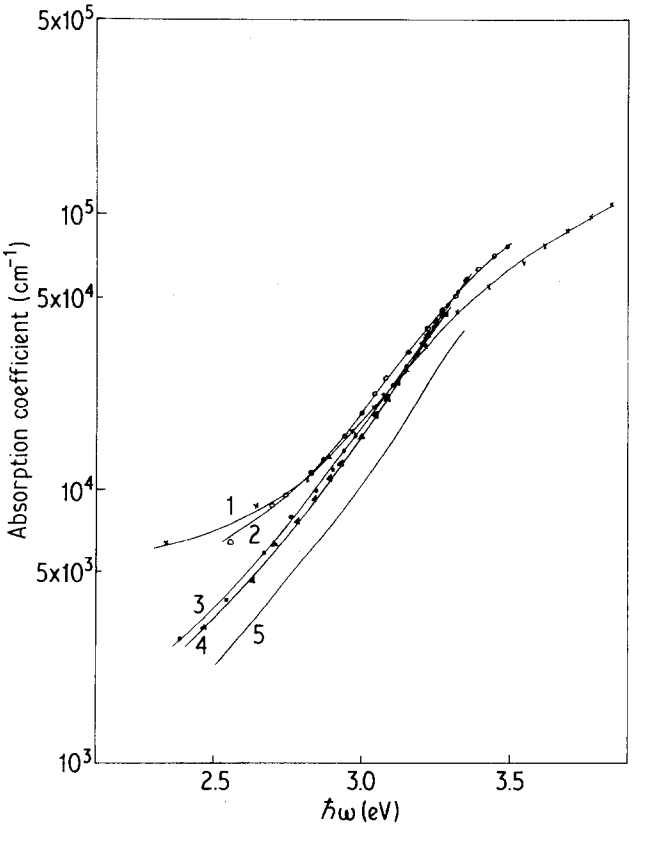

Figure 8 Absorption coefficient as a function of photon energy for more slowly evaporated SiO films. (Data of Fig. 4)

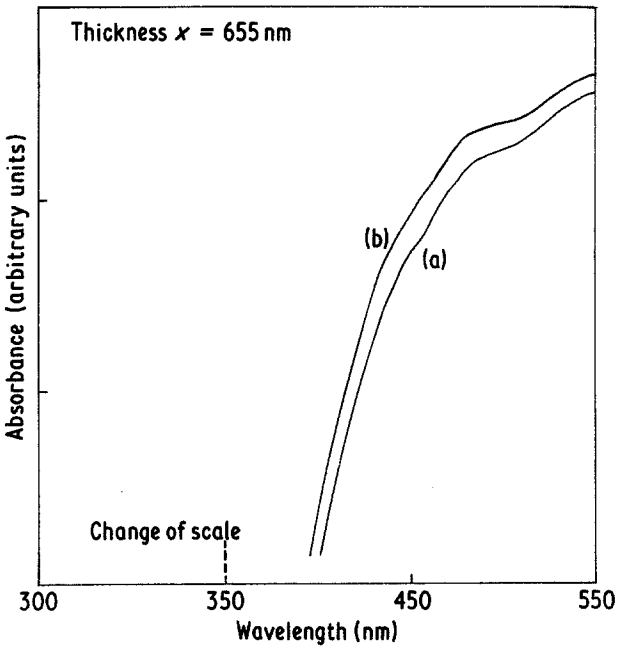

Figure 9 The form of the absorption edge for a rapidly evaporated thin SiO film: (a) as-evaporated; (b) after annealing.

of spin density with R/p. As is seen in Fig. 12, there is a correlation between the spin density and therefore between the density of the unsaturated bonds and the composition of the material. For a SiO_2 film where the parameter R/p is low, a density of $\sim 10^{18}$ spin cm^{-3} was observed. For higher values of the parameter R/p where it corresponds to a sample composition approximating to SiO, the absorbed signal was $\sim 10^{20}$ spin cm^{-3}. Three of these samples were annealed in vacuum for 4 h at a temperature of $\sim 200^{\circ}$ C and showed a significant reduction in the value of spin density of about 25%. This is in agreement with some trends found by Timson [18], that when the temperature of the substrate is reduced from 150° C to 40° C, an increase of ~20% in the value of spin concentration was detected, arising from the increased disorder in the sample. The variation of the refrac-

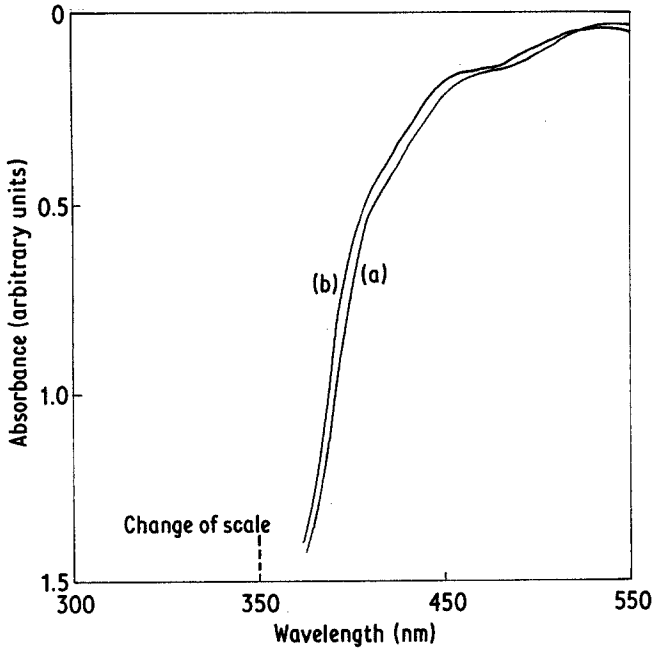

Figure 10 The form of the absorption edge for a more slowly evaporated thin SiO film: (a) as-evaporated; (b) after annealing.

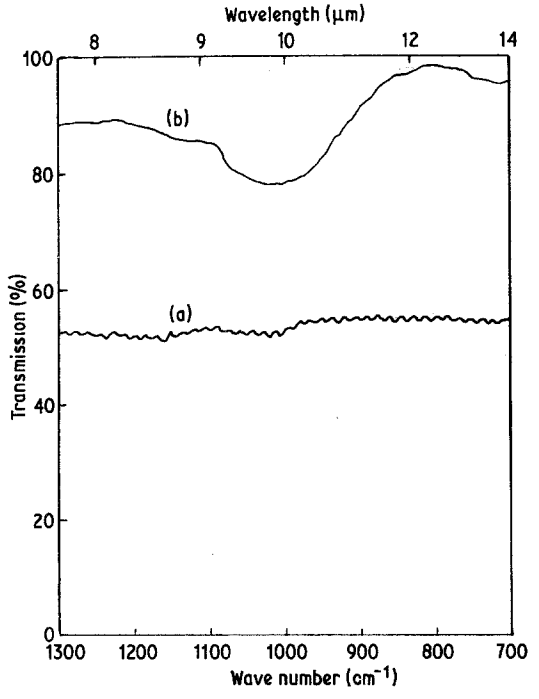

Figure 11 Absorption spectrum of thin SiO film evaporated at $R/p \simeq 10^7$ nm sec^{-1} torr^{-1}. (a) KBr substrate, (b) SiO film on KBr substrate.

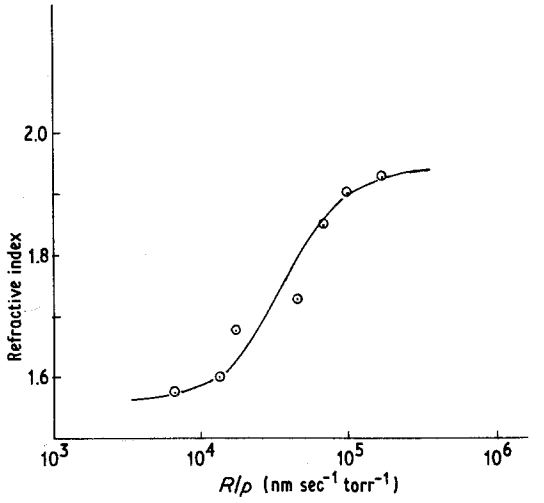

Figure 13 Variation of refractive index for silicon oxide films as a function of the parameter R/p.

tive index n with the parameter R/p is presented in Fig. 13. For high values of R/p the value of n is ~ 1.95, whereas for low values of R/p, n is ~ 1.6. This supports the results in Fig. 12 and is in good agreement with previous investigations [14].

The optical dielectric constant plotted against R/p is shown in Fig. 14. This value varies between 2.45 to 3.75 and lies within the range of dielectric constants for many thin oxide materials in the optical frequency range. Furthermore, studies on the dependence of the optical absorption and of E_{opt} on the parameter R/p were carried out by using the Perkin–Elmer spectrometer, as shown in Figs. 15a and b and 16. Fig. 15a shows the dependence of the absorbance as a function of the wavelength for samples having different values of R/p, while Fig. 15b shows a plot of $(\alpha\hbar\omega)^{1/2}$ as a function of the photon energy $\hbar\omega$ for the same values of R/p as are shown in Fig. 15a. This shows a variation in the values of optical energy gaps. For high values of R/p the energy gap is $\sim$ 2.45 eV which

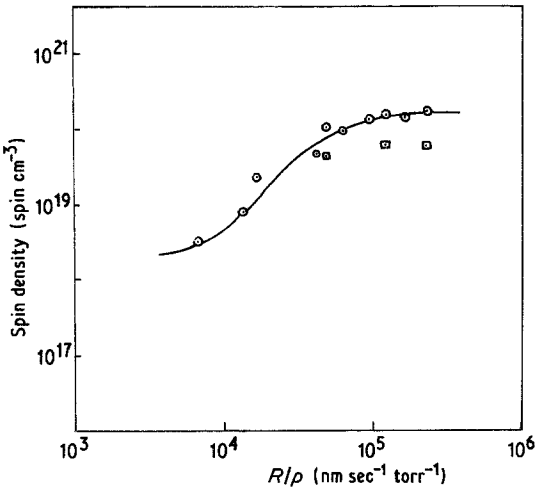

Figure 12 Electron spin density of silicon oxide films as a function of the parameter R/p (□ Sample annealed for 4 h at 200° C.)

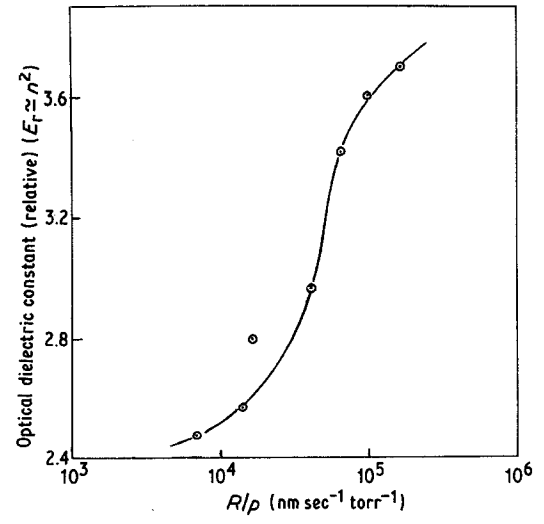

Figure 14 Optical dielectric constant as a function of R/p.

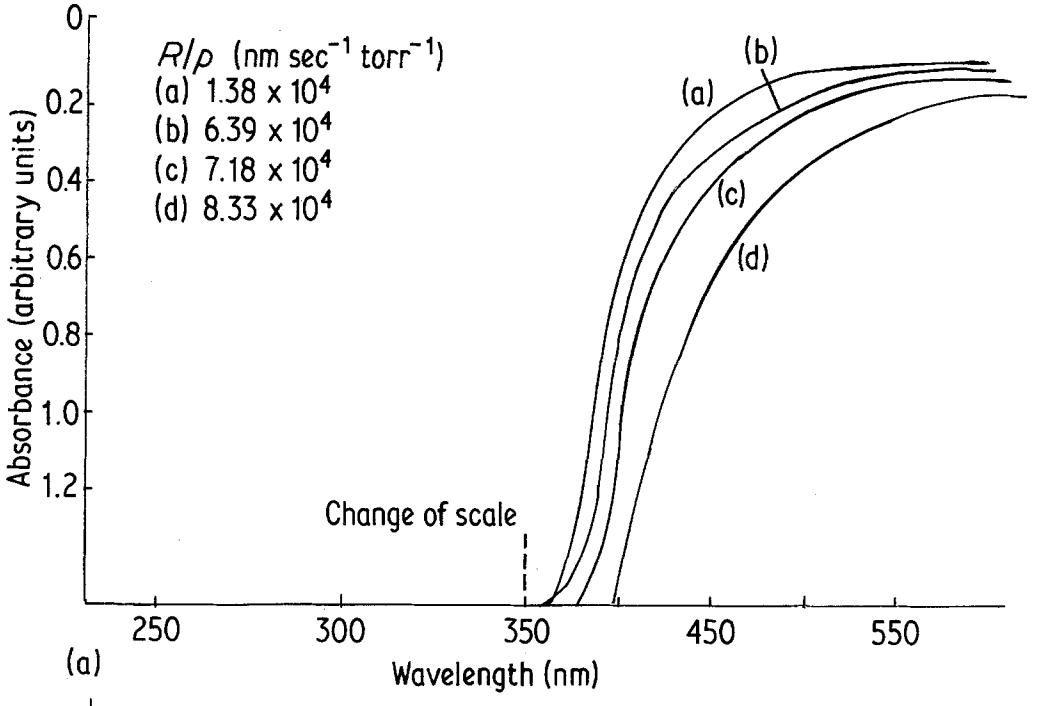

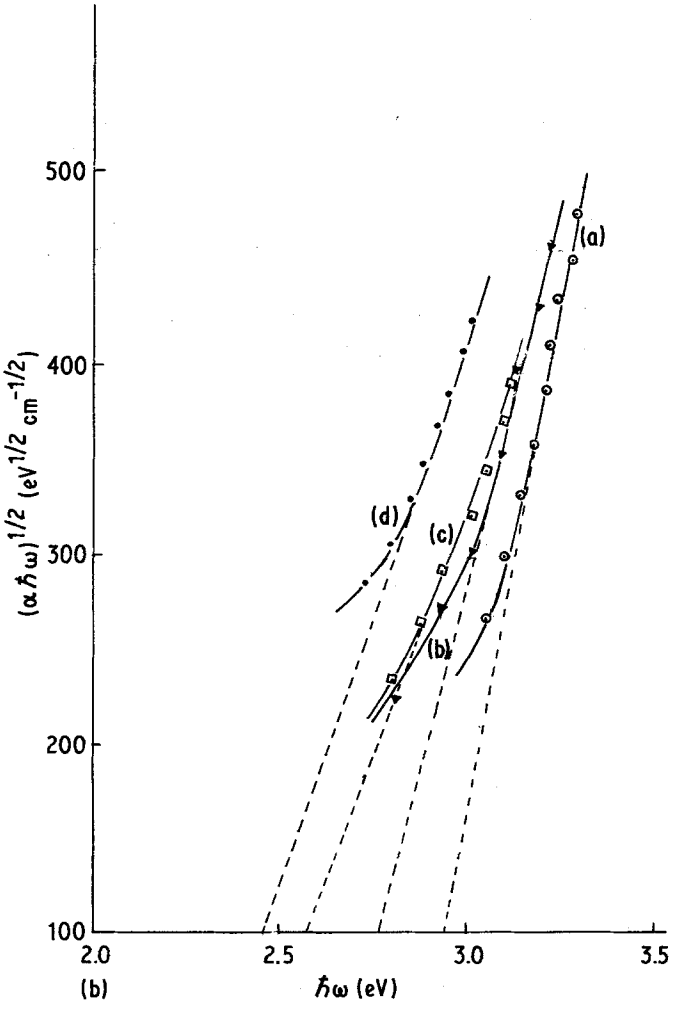

Figure 15 (a) Absorbance as a function of wavelength for samples deposited at different values of R/p. (b) Data of (a) replotted according to Tauc and to Davis and Mott.

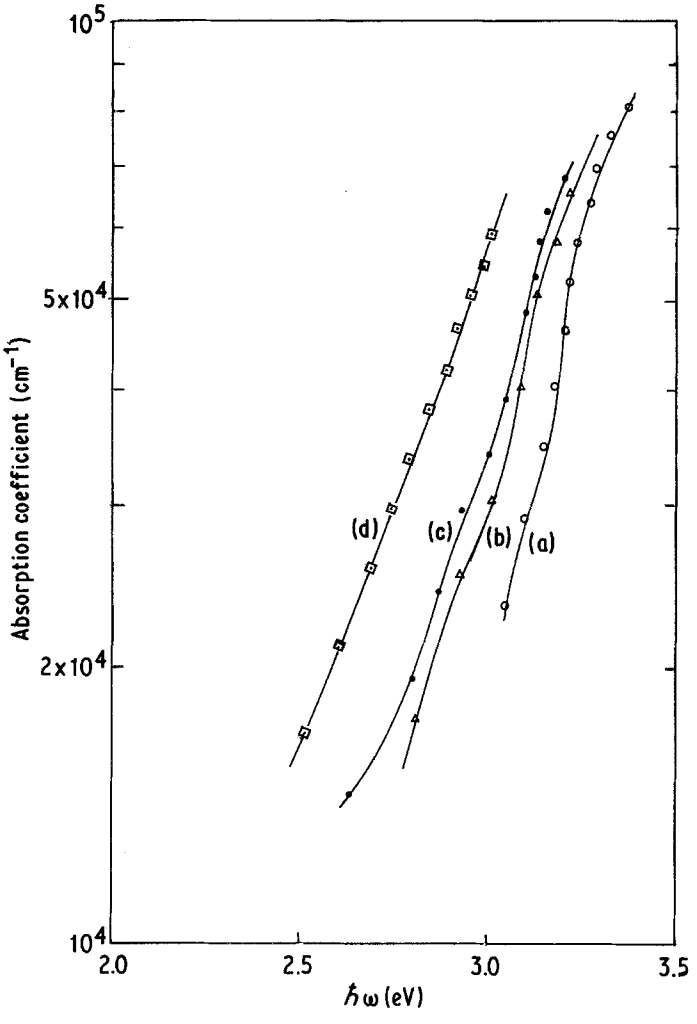

Figure 16 Data of Fig. 15a plotted to show up the Urbach rule.

corresponds predominantly to SiO, whereas the value of the energy gap reaches 2.94 eV for low values of R/p ($\sim 1.38 \times 10^4$ nm sec^{-1} torr^{-1}) which tends to the composition SiO_2. These values of optical energy gap and their dependence on R/p may be closely compared with the variation of the spin concentration with R/p which is given in Fig. 12, and the variation of refractive index n with R/p given in Fig. 13. Fig. 16 shows how the absorption coefficient is related to the photon energy for different values of R/p.

References

1. J. TAUC, *Mat. Res. Bull.* **5** (1970) 721.
2. E. A. DAVIS and N. F. MOTT, *Phil. Mag.* **22** (1970) 903.
3. J. TAUC, A. ABRAHAM, L. PAJASOVA, R. GRIGOROVICI and A. VANCU, Proceedings of the International Conference on Physics of Non-crystalline Solids, Delft, Holland, July 1964 (North-Holland, Amsterdam, 1965) p. 606.
4. J. TAUC, R. GRIGOROVICI and A. VANCU, *Phys. Status Solidi* **15** (1966) 627.
5. F. URBACH, *Phys. Rev.* **92** (1953) 1324.
6. J. TAUC, A. MENTH and D. L. WOOD, *Phys. Rev. Lett.* **25** (1970) 749.
7. N. F. MOTT and E. A. DAVIS, "Electronic Processes in Non-crystalline Materials" (Clarendon Press, Oxford, 1971).
8. G. R. MORIDI and C. A. HOGARTH, Proceedings of the International Conference on Amorphous and Liquid Semiconductors, Edinburgh, June 1977, edited by W. E. Spear (Centre for Industrial Consultancy, Edinburgh, 1977) p. 688.
9. C. A. HOGARTH and M. Y. NADEEM, *Phys. Status Solidi (a)* **68** (1981) K181.
10. G. HASS and W. R. HUNTER, in "Physics of Thin Films", Vol. 10, edited by G. Hass and M. H. Francombe (Academic Press, New York, 1978) p. 71.
11. A. HJORTSBERG and C. G. GRANQVIST, *Appl. Opt.* **19** (1980) 1694.
12. J. BEYNON, *Vacuum* **20** (1970) 293.
13. H. R. PHILIPP, *J. Phys. Chem. Solids* **32** (1971) 1935.
14. P. A. TIMSON and C. A. HOGARTH, *Thin Solid*

Films **8** (1971) 237.
15. S. CHAUDHURI, S. K. BISWAS, A. CHOUDHURY and K. GOSWAMI, *J. Non-cryst. Solids* **46** (1981) 171.
16. E. RITTER, *Opt. Acta* **9** (1962) 197.
17. J. TAUC, "Optical Properties of Solids", edited by F. Abelés (North Holland, Amsterdam, 1971) p. 277.
18. P. A. TIMSON, PhD Thesis, Brunel University (1971).

Received 5 August
and accepted 13 September 1983